◇論 文◇

Development of the World's Highest Strength Cementitious Material

世界最高強度セメント系材料の開発

KONO, Katsuya*;　NAKAYAMA, Risa*;
TADA, Katsuhiko**

河　野　克　哉*，中　山　莉　沙*，
多　田　克　彦**

要　　旨

本研究では，硬化モルタルにおいて最高の圧縮強度を達成することを目的として，新しいセメント系結合材に対する製造方法について検討した．３成分系セメント結合材の粒子径と組成について，Furnas の最密充填理論を用いて算出した．この材料で打ち込まれた供試体は，きわめて少ない水量の練混ぜによって製造される．そのため，最密粒度セメント系結合材を用いた脱型直後の硬化体に外部から水分を吸収させ，その後に二段階の熱養生を実施した．その結果，最密充填粉体設計と事前吸水処理によって，460N/㎜^{2} を超える圧縮強度を発現するセメント硬化体を得ることができた．

キーワード：超高圧縮強度，最密充填，事前吸水処理，熱養生

*中央研究所 第２研究部 ＴＢＣﾁｰﾑ　TBC Team, Central Research Laboratory
**中央研究所 第２研究部 ＴＢＣﾁｰﾑ ﾘｰﾀﾞｰ　Manager, TBC Team, Central Research Laboratory

ABSTRACT

In this study, new manufacturing methods have been investigated for cementitious materials containing novel cement systems. The purpose of this work was to achieve the highest level of compressive strength in hardened mortar. The grain size and proportions of ternary blended cement systems were calculated using the closest packing theory of Furnas. The cast specimens were prepared by mixing the constituents with an extremely small amount of water. After removal from the mold, the hardened products with the densest packing cement systems were subjected to water absorption from the outside surface, followed by two-stage heat curing. As a result, the densest packing design and pre-soaking treatment enable the production of hardened cement having ultra high compressive strength of more than 460N/mm^2.

Keywords : *Ultra high compressive strength, Closest packing, Pre-soaking treatment, Heat curing*

1. INTRODUCTION

Ultra high strength concrete is a material that enables higher reinforced concrete buildings and longer civil engineering concrete structures, and as shown in **Fig.1**, there is competition in the development of its strength. Since the company commenced sale of Ductal® (ultra high strength fiber reinforced concrete) in 2000, our technology for precast concrete with a compressive strength of 200 N/mm^2 has become the fastest spreading in Japan. Also in 2006 we launched SFPC® (silica fume premix cement) which develops a compressive strength of 80 to 150 N/mm^2, and in 2010 we developed SFPC200® (silica fume premix cement) which develops a compressive strength of 200N/mm^2, which established ultra high strength ready mixed concrete technology. However, thereafter the competition for development of ultra high strength concrete intensified within Japan, and in 2013 the highest design strength concrete in Japan of 300 N/mm^2 was developed as a precast member by another company[1]. Note that reactive powder concrete that develops a compressive strength of 673N/mm^2 was developed in France in 1994[2], and this is currently the highest strength ever recorded in the world. However, this overseas technology was achieved using a special method known as the hot press molding method (temperatures 250 to 400°C) as shown in **Fig.2(a)**, a method that is applied to the manufacture of fine ceramics. The method is not practical as it sacrifices the major advantage of concrete that it enables any shape to be obtained by assembling formwork and pouring. Therefore in this research the constituent materials, mixes, and production methods were studied with the objective of achieving concrete with the highest compressive strength that could be expected to be commercialized by normal pour molding into formwork as shown in **Fig.2(b)**.

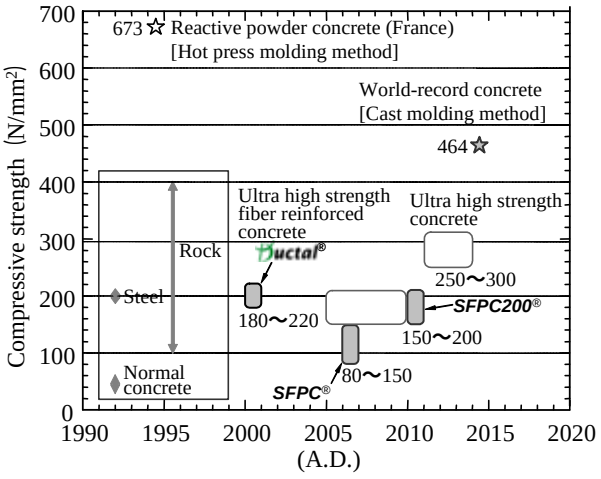

Fig. 1 The competition to develop ultra high strength concrete in Japan

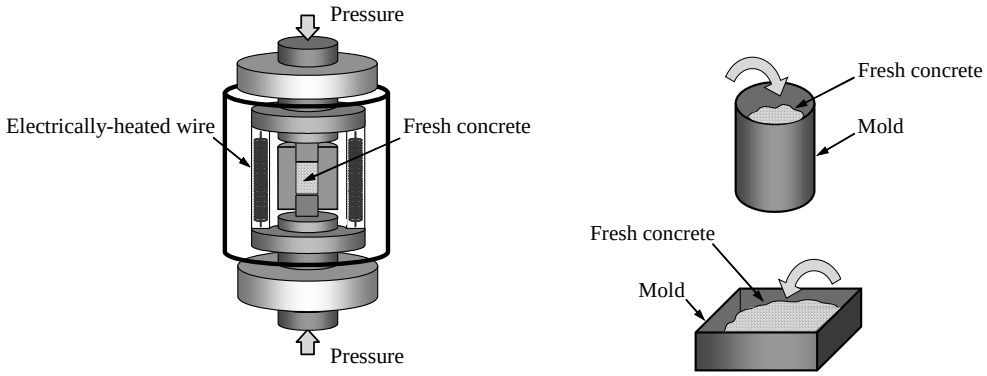

(a) Hot press molding method (b) Pour molding method

Fig. 2 Casting method for fresh concrete

Table 1 Materials

Material	Type	Symbol	Characteristics
Binder (B)	Low-heat Portland cement	LC	Specific surface area of 3330cm^2/g, Density of 3.24g/cm^2
	Quartz powder	QP	Density of 2.59g/cm^2
	Silica fume	SF	Specific surface area of 20m^2/g, Density of 2.29g/cm^2
Fine aggregate	Silica sand	S	Maximum size of 0.3mm, Density of 2.29g/cm^2
Chemical admixture	Superplasticizer	SP	Polycarboxylic acid type
	Defoaming agent	DFA	Polyether type (Polyalkylene glycol)

Table 2 Mix proportions

No.	W/B (%)	Unit contents (kg/m^3)							Flow (mm)	Air content (%)
		W	B			S	SP *	DFA *		
			LC	QP	SF					
1	13	180	913	362	107	927	B× 2.5%	B× 0.02%	230	2.2
2	15	199	876	347	102				295	2.0

* Replacement as a part of unit water content.

2. TEST METHODS

2.1 Materials, mix proportions, and mixing used

(1) Materials used

As shown in **Table 1**, low heat Portland cement (hereafter, LC), fine quartz powder (hereafter, QP), and silica fume (hereafter, SF) were used as the binder (hereafter, B). Also silica sand (hereafter, S) was used as the fine aggregate, and a superplasticizer (hereafter, SP) and a defoaming agent (hereafter, DFA) were used as chemical admixtures.

(2) Mix proportions

The mix proportions were as shown in **Table 2**. Here the method of processing the binder materials in order to obtain the maximum density grading was investigated, with the objective of obtaining a powder mixture that can flow with a small quantity of water (hereafter, W) by reducing as much as possible the gap between particles of each of the powders from which B was formed. In other words, the densest packing state of a discontinuous particle size distribution system of 2 to 4 powder components was calculated based on the densest packing theory of Furnas[3], which

is a convenient calculation method for given number of components, particle size, and ratio of size. In this calculation method, if the number of powder components is n+1, the void ratio of each powder is ε (assumed to be the same), the maximum particle size is D_1, the minimum particle size is D_{n+1}, the ratio of size of the maximum particle size and the minimum particle size $K = D_{n+1}/D_1$, and the particle size ratio of adjacent particles in the maximum density system $D_{n+1}/D_n = K^{1/n}$, the maximum density for 2, 3, or 4 components of powder is obtained for mixing proportions (volume ratio) of the n+1 components, Primary particle : secondary particle : tertiary particle : quaternary particle

$= 1/(1+\varepsilon) : \varepsilon/(1+\varepsilon) : \varepsilon^2/(1+\varepsilon) : \varepsilon^3/(1+\varepsilon)$

each term being divided by the sum total up to the $(n+1)^{th}$ particle.

Here, for the LC and SF powders shown in **Table 1**, when it is assumed that the average particle sizes are D_1 = 20 μm and D_3 = 0.1 μm respectively, and the void ratios are $\varepsilon_1 = \varepsilon_3 = 0.5$, the ratio of size $K = D_3/D_1 = 5\times10^{-3}$, from the relationship between the number of components and the ratio of size to give the maximum density for the powder mixture shown in **Fig.3**, the number of components to give the maximum density is n+1 = 3.05, so that means 3 components. In addition from the relationship $D_{n+1}/D_n = K^{1/n}$, the particle size that should be provided between LC and SF is calculated to be $D_2=(D_1.D_3)^{1/2}$ = 1.41 μm. The powder particle size of QP shown in **Table 1** (particle size D_2=1.41 μm, void ratio ε_2 = 0.5) was adjusted to be this intermediate particle, and the mixing proportions of each powder LC : QP : SF = 5.71 : 2.86 : 1.43　6 : 3 : 1 (volume ratio) for the 3 component binder, and two criteria for water binder ratio (hereafter, W/B) of 13% and 15% were used. For each mix the absolute volume of S was 355 L/m³, the percentage of SP added was B×2.5%, and the percentage of DFA added was B×0.02%.

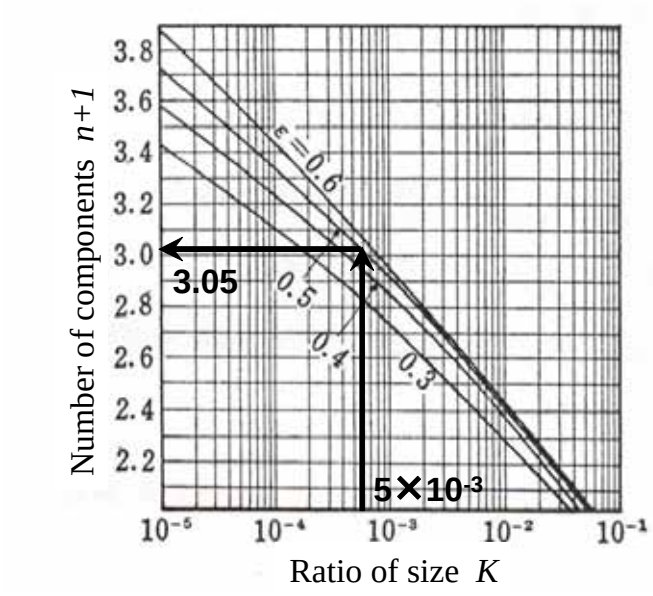

Fig. 3　Relationship between the number of components and the ratio of size to give the maximum density for the powder mixture

(3) Mixing

The B, W, SP, S, and DFA were placed in an omni-mixer (capacity 5 L), mixed for 6 minutes, and the mixed mortar was poured into a form (internal dimensions ϕ50×100 mm). Note that as shown in **Table 2**, in the range W/B = 13 to 15 % the consistency of the flow was in the range 230 to 295 mm, and the air content was 2.0 to 2.2 %, indicating that each mix had high fluidity to enable normal pour molding.

2.2　Water soaking and heat curing

(1) Water soaking

After pouring into a normal mold (internal dimensions ϕ50×100 mm), the test specimens that were cured in a sealed condition (at room temperature 20°C) up to an age of 48 hours were removed from the mold, and subject to deairing water absorption or boiling water absorption as described below.

i) As shown in **Fig.4(a)**, with the test specimens completely immersed in water within a closed vessel, water was supplied from the external surface to the interior of the test specimen by reducing the pressure by evacuating the top layer air using a vacuum pump. The deaeration duration was varied to 4 levels: 0 minutes, 1 minute, 30 minutes, and 90 minutes. Also, the test specimens were weighed before and after the deairing water absorption, and the quantity of water absorbed (V_w) was calculated.

ii) As shown in **Fig.4(b)**, with the test specimens completely immersed in water in an open vessel,

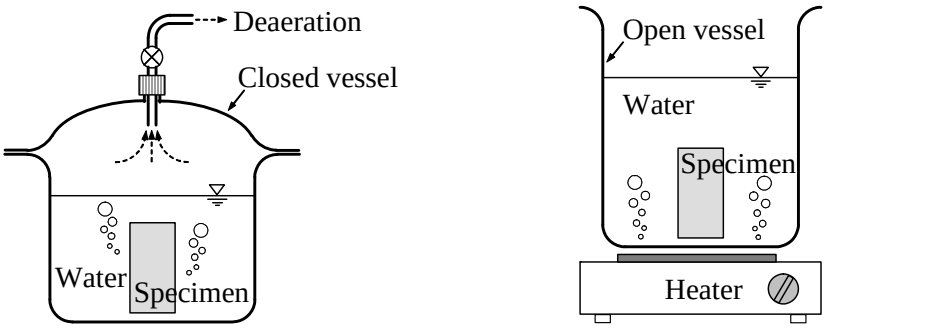

(a) Deairing water absorption method (b) Boiling water absorption method

Fig. 4 Pre-soaking treatment for test specimens just after removal mold

the temperature was raised at about 5°C per minute using an electrical heater until 100°C was reached, and boiling was continued for 30 minutes. Then the test specimens were cooled naturally in water to room temperature 20°C. Note that the test specimens were weighed before and after the boiling water absorption, and the quantity of water absorbed (V_w) was calculated.

(2) Heat curing

The test specimens that had been subjected to the water absorption process of i) or ii) were steam cured (rate of rise in temperature 15°C/h, maximum temperature 90°C, duration at maximum temperature 48 hours, rate of reduction in temperature 15°C/h, 1 atm), then heating curing was carried out (rate of rise in temperature 60°C/h, maximum temperature 180°C, duration at maximum temperature 48 hours, rate of reduction in temperature 60°C/h, 1 atm).

2.3 Test items

(1) Compressive strength tests

The compressive strength of the test specimens (dimensions ϕ50×100 mm) that had completed the 2 stage heat curing was measured using a compression machine (capacity 1,000 kN) in accordance with JIS A 1108 “Method of test for compressive strength of concrete”.

(2) Analysis of the composition of the hardened material

Test specimens (W/B = 15%) whose length was cut in half using a cutter after pouring into the mold (dimensions ϕ50×100 mm) and removal from the mold were subjected to deairing water absorption for 30 minutes or to boiling water absorption for 30 minutes immediately after removal from the mold as described in Section **2.2(1)**, and then subjected to 2 stage heat curing as described in Section **2.2(2)**. Also the bottom surface in contact with the mold and the finished surfaces after pouring were ground immediately after removal from the mold. Test specimens of dimensions 25×25×5 mm were cut from these test specimens as shown in **Fig.5**, impregnated with resin, ground, and subjected to carbon vapour deposition to provide thin specimens for

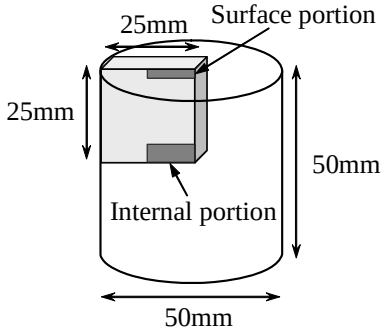

Fig. 5 EPMA specimens prepared by cutting the heat cured specimens

observation. Ten backscattered electron images using an electron probe micro-analyzer were obtained at both the surface portion of the thin specimens (in a range up to a depth of 1 mm from the surface) and the interior portion (in a range of depth 15 to 20 mm from the surface). The gray level of the backscattered images depends on the average atomic number of the observed image, so by binarization (a process that converts an image with contrasting density into 2 tones of black and white) of pixels occupied by unhydrated cement or a void, area regions were extracted as a detection image, and the respective volume percentages (percentage content) were calculated from stereology theory (in stereology theory the area percentage is equal to the volume percentage). For comparison the same backscattering electron image observation and image analysis was carried out on test specimens that were not subjected to water absorption immediately after removal from the mold.

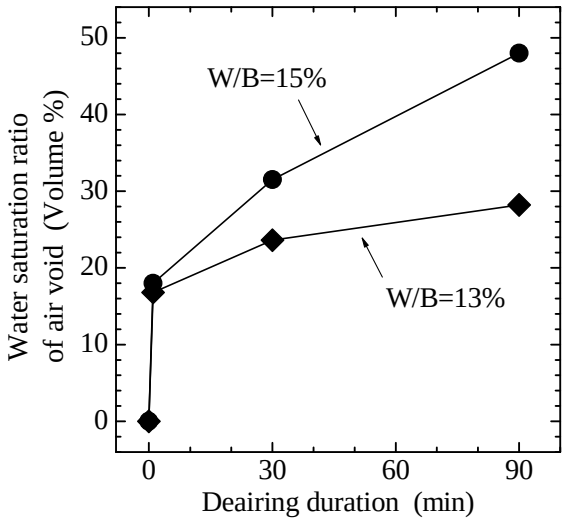

Fig. 6 Relationship between the water saturation ratio of air void and the deairing duration for test specimens subjected to deairing water absorption after removal from mold

(3) Hardened material micropore size stribution

Using test specimens (dimensions ϕ50×50 mm) produced under the same conditions as described in Section **2.3(2)**, test specimens of about 5 mm square were cut from the surface portion (the range up to a depth of 5 mm from the surface) and the interior portion (a range of depths from 15 to 20mm from the surface), and the pore size distribution was measured using a mercury penetration porosity meter.

3. TEST RESULTS AND DISCUSSION

3.1 Effect of deairing water absorption on the hardened cement material

(1) Water saturation ratio of air voids in test specimens

Fig.6 shows the relationship between the water saturation ratio of air voids and the deairing duration for test specimens that were subjected to deairing water absorption immediately after removal from the mold. The water saturation ratio of air voids (quantity of absorbed water V_w) is the quantity of water as a percentage of the voids in the test specimen obtained by multiplying the air content of the fresh mortar (a) shown in **Table 2** by the test specimen volume (V_m) ($V_w/(V_m.a)\times 100$) . In both cases of W/B = 13% and W/B = 15%, the longer the deairing duration the higher the water saturation ratio of air voids, and for the same deairing duration the water saturation ratio of air voids was higher for W/B = 15% than for W/B = 13%. In particular when the deairing duration was 30 minutes or higher, the water saturation ratio of air voids further increased for W/B = 15%, although it virtually peaked for W/B = 13%. It is considered that this was because the higher the W/B the coarser the microstructure of the hardened material when removed from the mold, so it still had a micro-structure with high water permeability, and water could be more easily absorbed from outside.

(2) Compressive strength of test specimens

Fig.7 shows the relationship between the compressive strength after heat curing and the deairing duration for test specimens subjected to deairing water absorption after removal from the mold. When the deairing water absorption was carried out for 30 minutes, the compressive strength was an average of 411 N/mm² for W/B = 13% and an average of 464 N/mm² for W/B = 15%, so it can be seen that for both values of W/B an extremely high compressive strength was

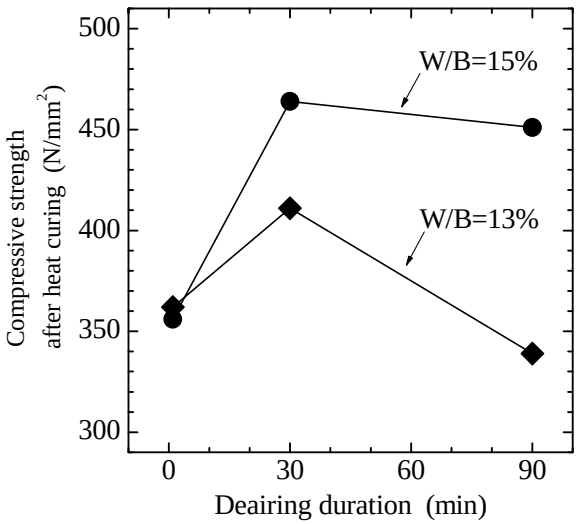

Fig.7 Relationship between the compressive strength after heat curing and the deairing duration for test specimens subjected to deairing water absorption after removal from mold

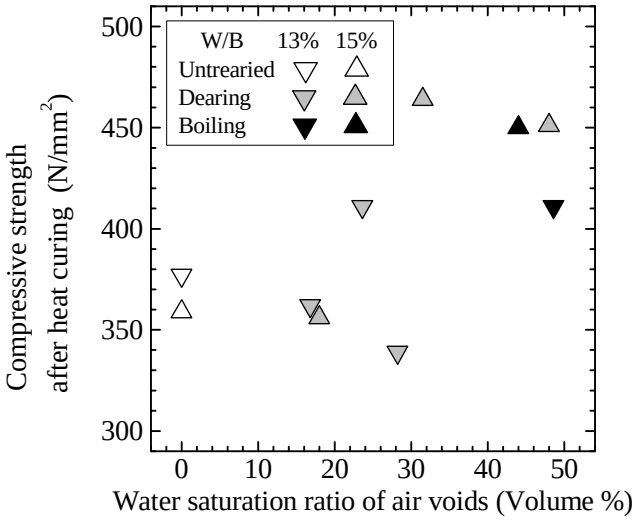

Fig.8 Relationship between the compressive strength after heat curing and the water saturation ratio of air voids for test specimens subjected to deairing water absorption or boiling water absorption after removal from mold

obtained. However, when deairing water absorption was carried out for 90 minutes, a reduction in compressive strength was seen for W/B = 13% compared with 30 minutes deairing water absorption, although for W/B = 15% the value was almost constant even though the deairing duration was extended. For short deairing durations of 0 minutes (water absorption not carried out) and 1 minute, there was no major difference in the compressive strength for W/B = 13% and W/B = 15%. In contrast when the deairing water absorption was carried out for 30 minutes or longer, the water saturation ratio of air voids of the test specimens was higher before the start of heat curing in the case of W/B = 15% compared with W/B = 13%, so an ultra high strength of 460 N/mm^2 or higher was obtained. This suggests that the water supplied from the outside surface to the interior of the test specimen immediately after removal from the mold functioned as reaction water during the subsequent heat curing. In other words, it is considered that the water forcibly absorbed from the outside was used for curing within the test specimen, and by contributing to the formation of an extremely dense hard microstructure, dramatically increased the compressive strength.

3.2 Effect of boiling water absorption on the cement hardened material

(1) Water saturation ratio of air voids in test specimens

Fig.8 shows the relationship between the compressive strength after heat curing and the water saturation ratio of air voids in test specimens for test specimens subjected to boiling water absorption after removal from the mold. In this figure the data for the test specimens subjected to deairing water absorption from **Figs. 6** and **7** is also shown for comparison. The water saturation ratio of air voids for the test specimens subjected to boiling water absorption for 30 minutes was 48.6% for W/B = 13% and 44.0% for W/B = 15%. In the case of boiling water absorption, substantially the same state of water saturation was achieved as for deairing water absorption, regardless of W/B. Also, for the W/B = 15% test specimens, when boiling was carried out for 30 minutes in water or when deairing was carried out for 30 minutes or more in water, in all cases the state was substantially the same, the voids of the test specimens being about half filled with water. As a result, it is considered that the voids within the test specimens that were subjected to steam pressure expansion due to the

boiling gradually absorbed water into the interior from the outside by the pressure reduction during natural cooling in the water.

(2) Compressive strength of test specimens

As shown in **Fig.8**, the test specimens that absorbed the water by boiling for 30 minutes had an average compressive strength of 411 N/mm^2 for W/B = 13% and 450 N/mm^2 for W/B = 15%. With boiling water absorption, the test specimen after removal from the mold is rapidly heated and experiences a 100°C environment at an early age, but achieves an extremely high strength after heat curing, so it is considered that initial defects such as temperature cracking, etc., due to internal constraint in the boiling and cooling process are not allowed to occur in the hardened microstructure.

3.3 Analysis of composition of hardened cement and the pore structure

(1) Unhydrated cement content

Fig.9 shows the backscattered electron images of the interior of the hardened material after heat curing for (a) test specimens subjected to deairing water absorption, (b) test specimens subjected to boiling water absorption, and (c) test specimens not subjected to water absorption after removal from the mold. The backscattered electron images display parts with heavy elements bright and parts with light elements dark, so it is also referred to as a composition image. In other words, unhydrated cement (legend: C) is displayed in light gray, hydrates (legend: H) are displayed in dark gray, and voids (legend: P) are displayed in black. From these images it can be seen that unhydrated cement is dispersed throughout

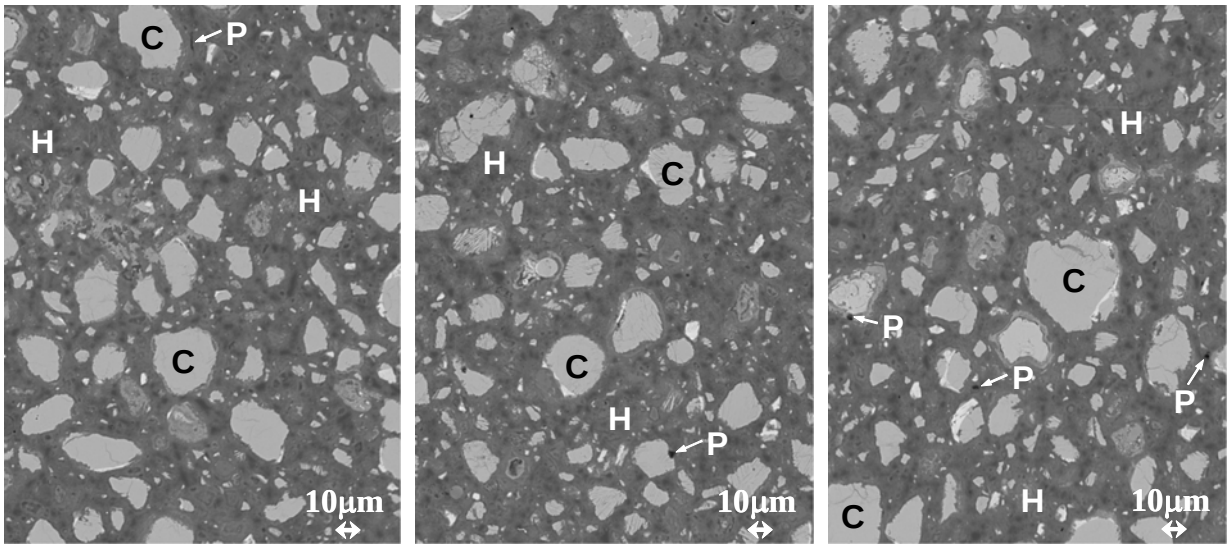

(a) With deairing water absorption (b) With boiling water absorption (c) Without water absorption

Fig. 9 Backscattered electron images of the internal of the hardened material after heat curing (C: Unhydrated cement, H: Hydrate, P: Air void))

Table 3 Calculated unhydrated cement content obtained by the backscattered electron image analysis for surface portion and internal portion of the hardened material

Type of pre-soaking treatment	Surface portion	Interior potion
With deairing water absorption	22.4 volume %	18.8 volume %
With boiling water absorption	21.0 volume %	16.9 volume %
Without water absoption	25.4 volume %	20.1 volume %

uniform continuous hydrates, and the voids that are displayed in black are extremely few. **Table 3** shows the calculated unhydrated cement content obtained by image analysis of the backscattered electron images for the surface portion and interior portion of the hardened material. It can be seen that by absorbing water by deairing or by boiling after removal from the mold, at both the surface portion and the interior portion the unhydrated cement content was reduced compared with when water absorption was not carried out. From this it can be deduced that the water absorbed into the interior after removal from the mold reacts strongly with the cement due to the heat curing, and forms a dense and hard microstructure.

(2) Pore size distribution

Fig.10 shows the pore size distribution at the surface and the interior of the hardened material subjected to the heat curing for test specimens subjected to deairing water absorption, test specimens subjected to boiling water absorption, and test specimens not subjected to water absorption. From this figure it can be seen that absorbing water after removal from the mold by deairing or boiling reduces the large pores both at the surface and the interior more than when water absorption is not carried out, and in addition the total volume of pores is reduced. In this way it is demonstrated that water absorption after removal from the mold causes refinement and reduction of pores in the hardened material, which contributes to achieving extremely high strength.

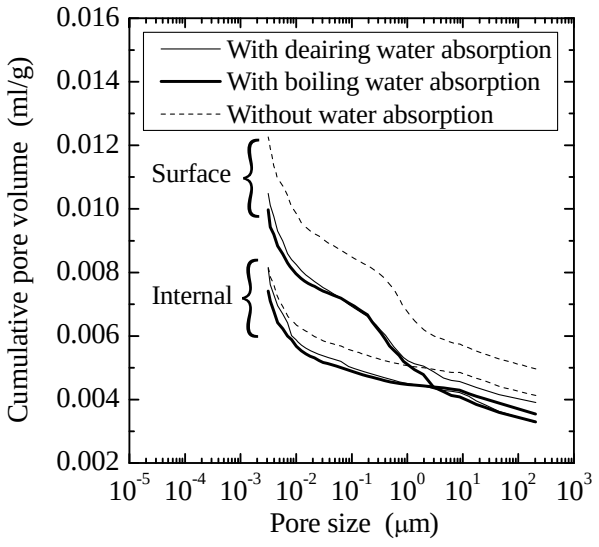

Fig. 10 Pore size distribution at the surface and the interior of the hardened material subjected to heat curing

4. CONCLUSION

In this research, an investigation was carried out into new materials and methods for producing hardened cementitious material with the aim of obtaining extremely high compressive strength by the normal method of pour molding into a mold. The following is a summary of the results obtained in this research.

(1) Fine quartz powder with average particle size adjusted to about 1.4 μm was added as an intermediate powder to a binder using low heat Portland cement and silica fume, and the mixing proportions of low heat portland cement : fine quartz powder : silica fume were set to 6 : 3 : 1 to provide a 3 component binder with the theoretically highest density particle size, and high fluidity to enable pouring into the mold was obtained at a low water binder ratio.

(2) Test specimens obtained by normal pour molding of the mortar obtained from the 3 component binder for the highest density particle size and a water binder ratio of 15% were subject to either deairing water absorption or boiling water absorption after removal from the mold, and water saturation ratio of air voids of about 50% was achieved.

(3) The test specimens that had been subjected to water absorption after removal from the mold were then given 2 stage heat curing (steam curing at a maximum temperature of 90°C and heat curing at a maximum temperature of 180°C), and it was possible to obtain a new hardened cement material that achieved a compressive strength of 450 to 464 N/mm², which is a new record by the normal pour molding method.

(4) The unhydrated cement content in the hardened cement material was reduced by the forcible water absorption by deairing or boiling after removal from the mold. In

addition, it was confirmed that large size pores were reduced and the total pore volume was reduced in the test specimens that were subjected to water absorption after removal from the mold. From this it is considered that the cement reactivity was increased by the heat curing after water absorption after removal from the mold, and the pores were filled with hydrates, which enabled an extremely high strength to be achieved.

REFERENCES

1) K. Imai; K. Yamamoto; M. Kato; A. Muramatsu. Development and application of slender RC columns using concrete with design strength of 300 N/mm². Concrete Journal. 2013,51(12),p.959-966 (in Japanese).
2) M. Uzawa; K. Yamada. Trends in development of ultra high strength high toughness concrete using RPC. Concrete Journal. 2001,39(2),p.53-56 (in Japanese).
3) C. C. Furnas. Grading aggregate –Mathematical relations for beds of broken solids of maximum density. Industrial and Engineering Chemistry. 1931,23(9),p.1052-1058.